Proceedings of 14th IOE Graduate Conference
Peer Reviewed
Year: 2023 Month: December Volume: 14
ISSN: 2350-8914 (Online), 2350-8906 (Print)

Reactive Power Compensation in PV-Wind Integrated Microgrid using PV-STATCOM

Saugat Regmi [a], Sandeep Dhami [b], Bhriguraj Bhattarai [c], Yogesh Layalu [d]

[a, b, c] *Department of Electrical Engineering, Pashchimanchal Campus, IOE, Tribhuvan University, Nepal*
[d] *Department of Electrical Engineering, Khwopa College of Engineering, Tribhuvan University, Nepal*
[a] saugat31@outlook.com, [b] sandeep.dhami@ioepas.edu.np, [c] bhrigurajbhattarai@gmail.com, [d] lyogesh2022@gmail.com

Abstract
The integration of renewable energy sources, such as photovoltaic (PV) and wind power, into microgrid systems has gained significant attention due to its potential to enhance energy sustainability and reliability. However, the intermittent nature of these sources introduces challenges related to voltage stability and reactive power management. This research focuses on addressing these challenges by proposing a novel approach to reactive power compensation using a PV-STATCOM (Static Synchronous Compensator) in a PV-Wind hybrid microgrid system. The objective of this study is to investigate the effectiveness of employing a PV-STATCOM to mitigate voltage fluctuations and improve power quality in the hybrid microgrid. The PV-STATCOM operates as a reactive power source, injecting or absorbing reactive power as needed, to regulate voltage levels and maintain optimal grid performance. To achieve this, advanced control strategies are developed and implemented, considering the unique characteristics of both PV and wind energy sources. The research methodology involves modeling the PV-Wind hybrid microgrid system in MATLAB/Simulink software, followed by the design of the proposed PV-STATCOM control strategy. The performance of the system is evaluated under various operating conditions, including fluctuating renewable energy generation (varying irradiance and wind speed) and dynamic load changes.

Keywords
Photovoltaic, Wind Plant, Microgrid, PV-STATCOM, Reactive Power, dynamic load changes

1. Introduction

The development of photovoltaic (PV) systems as a viable renewable energy source has been driven by the need to mitigate climate change and reduce dependence on fossil fuels. PV technology directly converts sunlight into electricity through the photovoltaic effect, which was first discovered by French physicist Alexandre-Edmond Becquerel in 1839. However, it was not until the mid-20th century that practical applications of PV systems began to emerge.

The advancement of PV technology can be attributed to several key milestones. In the 1950s, researchers at Bell Laboratories developed the first practical silicon-based solar cell, marking a significant breakthrough in PV technology [1]. The subsequent refinement of silicon solar cell manufacturing processes and the introduction of thin-film solar cells in the 1970s further expanded the possibilities of PV applications. The 21st century witnessed substantial growth in the PV industry, driven by declining costs, increased efficiency, and supportive government policies. The introduction of innovative PV cell designs, such as multi-junction cells and perovskite-based cells, has further enhanced the efficiency of PV systems [2]. Furthermore, advancements in PV module manufacturing techniques, such as the use of automated production lines and improved material utilization, have contributed to cost reductions. The deployment of PV systems has witnessed remarkable growth globally, with both utility-scale installations and distributed generation systems contributing to the expansion of solar capacity. In recent years, PV installations have experienced significant cost reductions, making solar energy increasingly competitive with conventional fossil fuel-based generation sources [3]. PV systems have proven to be versatile and adaptable, capable of being deployed in various settings, including residential, commercial, and utility-scale applications. They offer numerous environmental benefits, including reduced greenhouse gas emissions, lower water consumption compared to conventional power plants, and minimal air and water pollution.

The integration of PV systems into the electricity grid presents both opportunities and challenges. Grid-connected PV systems can supply clean electricity to the grid, contributing to the decarbonization of the power sector. However, the intermittent nature of solar energy requires effective grid integration and energy storage solutions to ensure a reliable and stable power supply.

The integration of renewable energy sources, energy effectiveness, and enhanced reliability are all issues that PV-integrated microgrid systems have attracted a lot of attention for potential solutions. These systems generate localized power systems that may function both linked to and separated from the primary electrical grid by integrating PV technology with microgrids. In the drive for more flexibility and resilience in the face of changing energy environments, the idea of microgrids has grown in significance. To meet local energy demand, microgrids enable the integration of various energy sources, such as PV systems, Wind energy system, energy storage, and other distributed energy resources (DERs). This enables lower transmission losses, greater penetration of renewable energy sources, and better power quality. The

addition of PV systems to microgrids has many benefits. PV energy reduces reliance on fossil fuels and greenhouse gas emissions by being a clean, abundant resource. Since PV modules can be installed on rooftops, in open spaces, or as building materials, they are suitable for distributed generation. During grid interruptions, PV systems' energy self-sufficiency and resilience increase the reliability of the microgrid [4].

In order to operate and control PV-integrated microgrids effectively, cutting-edge technologies are utilized. The components of these systems include communication networks, energy management systems, intelligent control algorithms, and power electronic converters. DC power from PV modules is transformed into AC power via power converters, such as inverters so that it can be synchronized with the grid or used in an isolated mode. Energy management systems monitor power quality, optimize energy flow, and coordinate the functioning of multiple DERs. Within the microgrid, control techniques enable effective control of power converters, regulating voltage, and load distribution.

In an electrical power system, STATCOM, or Static Synchronous Compensator, provides voltage control, reactive power compensation, and improved system stability by using the flexible AC transmission system (FACTS) [5]. The system works using power electronics and voltage source converter (VSC) technology, incorporating capacitors, inductors, and power electronic switches such as insulated-gate bipolar transistors (IGBTs) [6]. Power systems of the past were predominantly linear, meaning that most loads followed sinusoidal waveforms in sync with the system voltage. In recent years, however, the use of power electronics and electronic devices has increased the presence of nonlinear loads. Current-voltage characteristics of nonlinear loads result in distorted waveforms.

In this paper, PV-STATCOM is implemented to compensate reactive power demand by reactive load. PV-Wind Hybrid model is developed, integrated with grid and active and reactive loads. Reactive load is compensated by PV-STATCOM instead of supplying from grid by developing the control strategy for PV-STATCOM.

2. System Modelling

2.1 PV-Array Modeling

This model can almost represent the essential characteristics of solar cell. The current source represent photocurrent generated by PV cell and this photocurrent is proportional to the intensity of light. The diode of the model represents the p-n junction of a PV Cell as it is made up of semiconductor material. The IV characteristics and non-linear response of the cell to changes in voltage and light intensity are represented by the diode. Figure 1 shows the equivalent circuit for a PV cell. To make it realistic, series and shunt resistors are placed as shown. The shunt and series resistances represent the resistive behaviour of PV Cells. The leakage current is represented by shunt resistance (Rsh) while the resistive losses in the cell's interconnection are represented by series resistance (Rs).

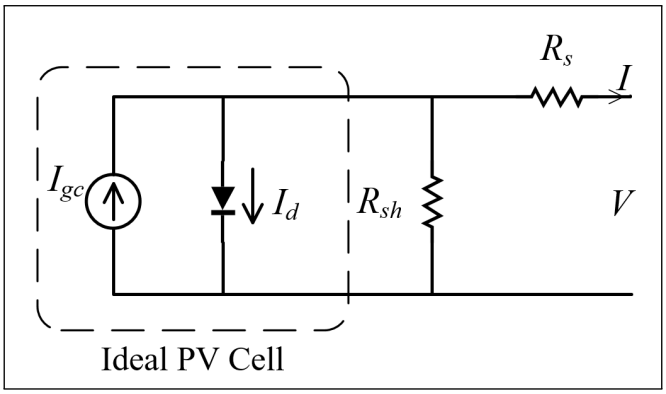

Figure 1: Equivalent model of PV Cell with shunt and series resistances

We know that the current-voltage relation of a PV cell is given by,

$$I_d = I_0 e^{\frac{V}{\eta V_T}} - 1 \tag{1}$$

Where I_d is the diode current, I_0 is the reverse saturation current of the diode, V is the voltage across the diode, η is the diode ideality factor, V_T is the terminal voltage which is given by,

$$V_T = kT/q \tag{2}$$

Where k is the Boltzmann constant, T is the temperature in Kelvin and q is the elementary charge. Applying Kirchhoff's current law,

$$I = I_{gc} - I_d \tag{3}$$

I_{gc} is photocurrent generated by PV cell and I is output current of cell. From the above equation,

$$I = I_{gc} - I_o \left[e^{\frac{V}{\eta V_T}} - 1 \right] \tag{4}$$

Considering the effect of series and shunt resistances, We can obtain,

$$I = I_{gc} - I_o \left[e^{\frac{V+IR_s}{\eta V_T}} - 1 \right] - \left[\frac{V + IR_s}{R_{sh}} \right] \tag{5}$$

Equation (5) is the required mathematical model of a PV cell.

2.2 DC-DC Boost Converter Modeling

To produce maximum power from solar plant, MPPT system is implemented in the project. Input capacitor stores energy to smoothen the output voltage curve. When switch is in ON condition, the input capacitor is charged. When switch is in OFF condition, capacitor is discharged. Maximum power point (MPP) occur when load resistance is equal to the source resistance. The input impedance depends on duty cycle and load resistance. To make load resistance and source impedance equal, source impedance is changed by changing duty cycle [7]. In order to maintain bus voltage at the output, a power electronic DC voltage regulator is required. PV system and load are connected via MPPT controller. Ripple signals are grounded through the shunt capacitor filter (C) which can be present in output of PV-Array.

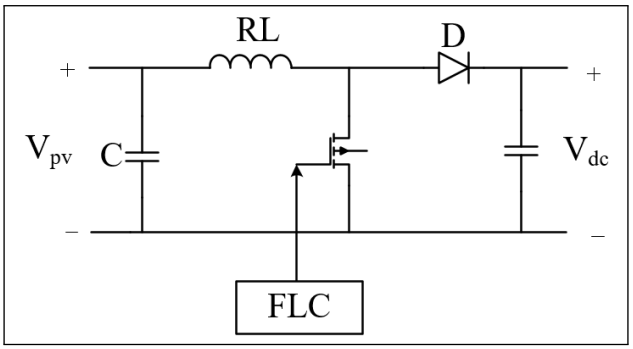

Figure 2: Boost Converter

Duty cycle (D) of converter is given as,

$$D = 1 - (V_{\text{in min}} \times \eta)/V_{\text{out}}) \tag{6}$$

Where,
$V_{\text{in min}}$ is minimum output voltage at rectifier output
V_{out} is converter output voltage
η is efficiency of converter

Output current (I_o) of converter is given as,

$$I_o = P_o/V_{\text{out}} \tag{7}$$

Where, P_o is output power of converter Considering 20% of output current as output ripple current, ripple current is given as,

$$I_{o\,ripple} = 0.2 \times I_o \tag{8}$$

Then, input current ripple is given as,

$$dI = I_{o\,ripple}\left[\frac{V_{\text{out}}}{V_{\text{in min}}}\right] \tag{9}$$

Again, considering 0.5% of output voltage as output ripple voltage, it is given as,

$$dI = I_{o\,ripple}\left[\frac{0.5}{100}\right] \tag{10}$$

Sizing of Inductor,

$$L = V_{\text{in min}} \times \left[\frac{V_{\text{out}} - V_{\text{in min}}}{dI \times f_s \times V_{\text{out}}}\right] \tag{11}$$

Where, f_s is the switching frequency considered as 20 kHz.

Sizing of Capacitor,

$$C = \frac{I_o \times D}{f_s \times dV} \tag{12}$$

$$R = \frac{V_{\text{out}}}{I_o} \tag{13}$$

2.3 Fuzzy Logic Controller

Fuzzy logic controller is implemented to generate gate pulse for the boost converter. By changing duty cycle of converter, input impedance is made constant to track maximum power point. The FLC process includes:

- Fuzzification
- Rule Evaluation
- Defuzzification

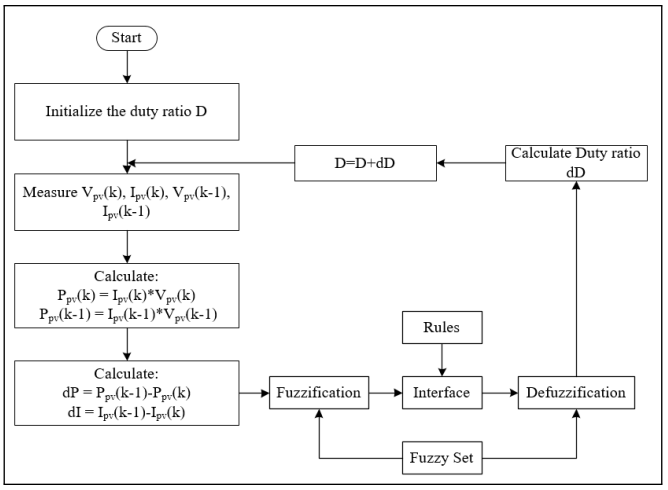

Figure 3: Fuzzy logic controlling for MPP

At first, in fuzzification, the crisp inputs are taken and converted to fuzzy input and assign them a fuzzy value according to the membership functions and rules. All the IF-THEN statements are called as rules. IF-THEN rules are used in the rule base that explain the connection between the input and output variables. Each rule uses linguistic expressions to specify an action (THEN part) and a condition (IF part). The controller assesses each rule in the inference and chooses the level of activation based on the degree to which the input values are members of the IF portion of the rule. In Defuzzification, the fuzzy output are converted into non-fuzzy output that can be useful for processing. An analog signal is generated in this defuzzification process to control the boost converter. The process of defuzzification utilizes the centroid method (a weighted average approach), commonly applied in FLC design due to its effective averaging characteristics and ability to yield favorable outcomes. In the project, a fuzzy logic controller with two input variables: change in power (dP) and change in current (dI) are taken while change in duty cycle (dD) is taken as output variable. Using the information from these two inputs, the Fuzzy Logic Controller determines the subsequent operational position based on the applied membership functions and a set of rules.

$$dP(k) = P(k) - P(k-1) \tag{14}$$

Where,

$$P(k) = V(k) \times I(k) \tag{15}$$

And,

$$dI(k) = I(k) - I(k-1) \tag{16}$$

Depending on the location of the operating point, the output variable (dD) can be either positive or negative and is sent to boost converter. This output variable is given as [8],

$$D(k) = D(k-1) + dD(k) \tag{17}$$

Four membership functions are used for dP, and dI input variable and dD output variable in the project. Four linguistic variables: Negative Big (NB), Negative Small (NS), Positive Big (PB) and Positive Small (PS) are those membership functions. Degree of membership range from 0 to 1. The range of input variable change of power (dP) range from -5 to 5, change of current range from -0.1 to 0 and output variable change of duty cycle range from -0.008 to 0.008.

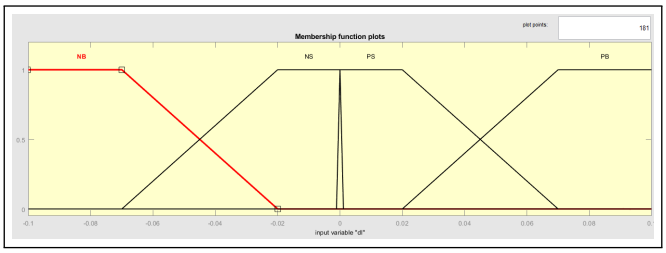

Figure 4: Membership functions of change in current

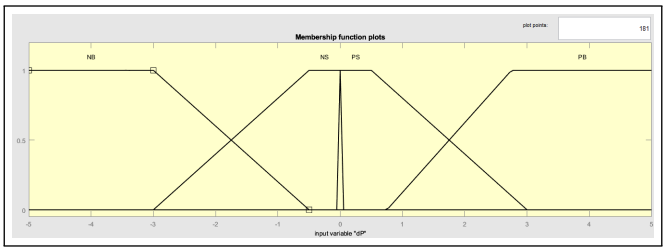

Figure 5: Membership function of change in power

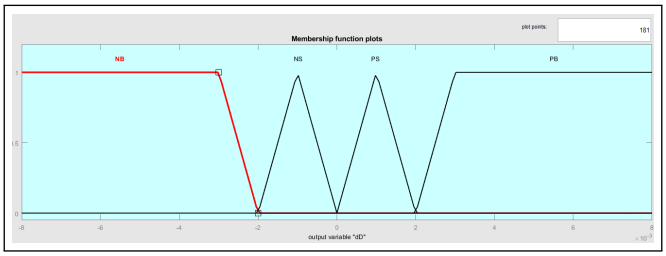

Figure 6: Membership function of change in duty cycle

Table 1: Fuzzy Rule

dD	dI	PB	PS	NB	NS
dP					
PB		PB	PB	NB	NB
PS		PS	PS	NS	NS
NB		NB	NB	PB	PB
NS		NS	NS	PS	PS

Four membership functions gives sixteen output. AND logical operation is implemented in the project. Change in current and power input variable are ANDed and change in duty cycle is determined. Syntax of these rules is as follow:

IF (dP is PB) and (dI is PB) THEN (dD is PB).

This principle indicates that when there's a change in power labeled as PB and a corresponding change in current also labeled as PB, it implies that the duty cycle needs to be increased by PB in order to raise the output voltage. The fuzzy rules created in the rule editor of MATLAB Simulink are presented below.

2.4 Voltage Source Converter

Voltage Source Converter consists of power semiconductor devices (IGBTs and MOSFETs). These switches are rapidly turned on and off to generate the required output. Controlling of these switches is done by gate signal which is generated by VSC Controller. VSC are self-commutated converters to connect HVAC and HVDC systems. Self-commuting VSCs are capable of generating AC voltages without relying on an AC supply. As a result, active and reactive power can be controlled independently and black starts (restoration of the electrical grid or power station after shutdown) are possible. It also can be used in PV plants as an inverter and reactive power compensator by controlling the gate signal, hence working as a PV-STATCOM.

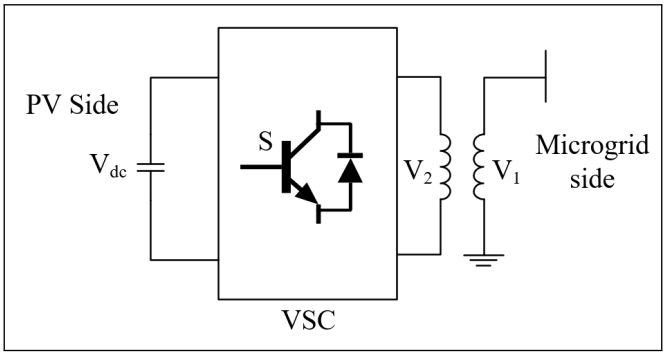

Figure 7: Voltage source converter working

PV-STATCOM supports reactive power in the microgrid. It is a voltage source converter (VSC) based FACTS. It improves voltage stability and harmonics of the system which is generated by non-linear and reactive loads. VSC either generates or absorbs the reactive power as per the requirement to maintain stability in the system. The variation of reactive power is performed by means of a Voltage-Sourced Converter (VSC). The VSC uses forced-commutated power electronic devices (GTOs, IGBTs, or IGCTs) to synthesize a voltage, V2, from a DC voltage source. In the figure, V1 represents the system voltage or gird voltage to be controlled and V2 is the voltage generated by the VSC. The model of PV-STATCOM is represented as,

$$P = \frac{V_1 V_2 \sin\delta}{X} \tag{18}$$

$$Q = \frac{V_1(V_1 - V_2\cos\delta)}{X} \tag{19}$$

Where, V_1 = System voltage to be controlled, V_2 = Voltage generated VSC, X = Reactance of the transformer, δ = Phase angle of V_1 w.r.t V_2

In steady-state operation, V2 is in phase with V1 (δ=0), so that only reactive power is flowing (P=0). If V2 is lower than V1, Q is flowing from V1 to V2 (PV-STATCOM is absorbing reactive power). On the reverse, if V2 is higher than V1, Q is flowing from V2 to V1 (STATCOM is generating reactive power).

2.5 Gate control of VSC

The three phase system abc is converted to two phase dq0 system to analyze the system with less complication. The abc to dq0 block is available in Simulink library and is used in the project at PLL and Measurement block.

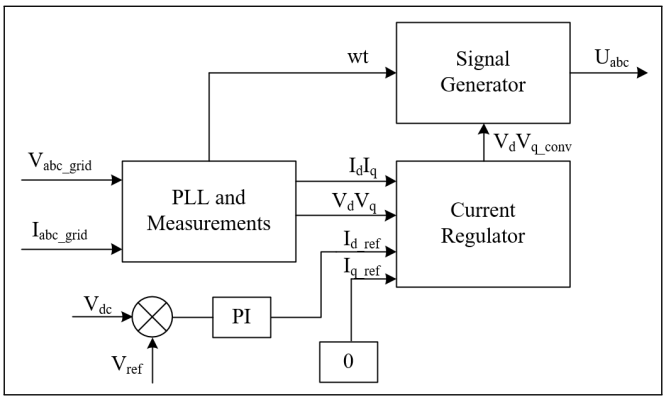

Figure 8: Gate control of VSC

abc to dq0 transformation is given as,

$$\begin{bmatrix} I_d \\ I_q \\ I_0 \end{bmatrix} = \sqrt{\frac{2}{3}} \begin{bmatrix} cos\theta & \cos\left(\theta - \frac{2\pi}{3}\right) & \cos\left(\theta - \frac{4\pi}{3}\right) \\ sin\theta & -\sin\left(\theta - \frac{2\pi}{3}\right) & -\sin\left(\theta - \frac{4\pi}{3}\right) \\ \frac{1}{\sqrt{2}} & \frac{1}{\sqrt{2}} & \frac{1}{\sqrt{2}} \end{bmatrix} \begin{bmatrix} I_a \\ I_b \\ I_c \end{bmatrix}$$

I_d is responsible for the generation of active power whereas I_q is responsible for the generation of reactive power. It is due to the magnetic tie up between stator and rotor pole produced by d-axis coil current [9].

In PLL block, the grid voltage, current and phase is measured along with abc to dq transformation. Iq_{ref} is set to zero while Id_{ref} is generated by comparing the DC link voltage and reference voltage. Current and Voltage in dq axis is fed to current regulator to generate converter voltage. In signal generator block, gate signal is generated considering phase, transformer correction factors, converter voltages, and DC link voltage. This generated signal is fed to VSC for controlling gates.

2.6 Wind Plant Modeling

A horizontal axis wind turbine and squirrel cage induction generator are implemented to generate wind power. The power generated by wind turbines is given as,

$$P_w = \frac{\pi \times \rho C_p R^2 v^3}{2} \tag{20}$$

Where, P_w = Mechanical power generated by wind turbine, ρ = air density (kg/m^3), R = Radius of blade, v = Velocity of wind, C_p = Power coefficient that represents the aerodynamic efficiency of blades at an operating point

C_p is the function of the speed ratio (λ) and pitch angle of the blade (β).

$$C_p(\lambda, \beta) = c_1(c_2 - c_3\beta^2 - c_4)e^{c_5} \tag{21}$$

The parameters c_1, c_2, c_3, c_4, and c_5 depend on the aerodynamic characteristics of the turbine. For a modern turbine these parameters are obtained empirically: $c_1 = 0.5$, $c_2 = \frac{R}{\lambda}$, $c_3 = 0.022$, $c_4 = 5.6$, and $c_5 = -(0.17\frac{R}{\lambda})$ [10].

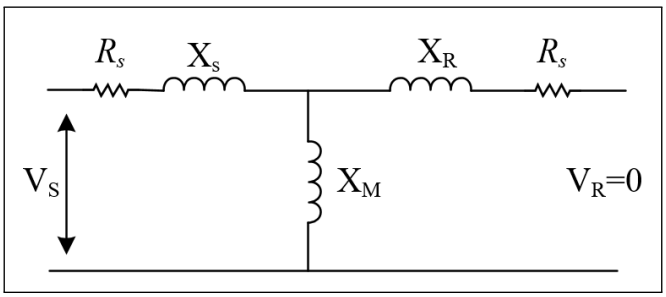

Figure 9: Equivalent Model of SCIG

Squirrel Cage Induction Generator equivalent circuit is shown in figure. The voltage equivalent is:

$$E = jI_mX_m = -I_r(R_r/s + jX_r) \tag{22}$$

$$I_m = I_s + I_r \tag{23}$$

$$V_s = E + I_s(R_s + jX_s) \tag{24}$$

$$P_{mec} = 3I_r^2(R_r/s) \tag{25}$$

Where,
E = Air gap magnetic field induction emf,
I_s = SCIG stator current ,
I_r = rotor current,
I_m = exciting current,
R_s = stator resistance,
R_r = Rotor resistance,
X_s = Stator secondary leakage reactance,
X_r = rotor secondary leakage reactance,
X_m = magnetizing reactance,
S = Slip

According to the voltage equivalent and variation range of s small in the real stable operation of wind power system,

$$V_s = I_r/(|s|X_m)k_s \tag{26}$$

$$k_s = \sqrt{M^2 + N^2} \tag{27}$$

$$M = -(sR_sX_r + sR_sX_m + X_sR_r + R_rX_m) \tag{28}$$

$$N = (R_sR_r - sX_rX_s - sX_mX_s - sX_rX_m) \tag{29}$$

$$V_s = k_r\sqrt{(v_r^3)/((v_s - v_r))} \tag{30}$$

From above equation we can model the SCIG and see that the terminal voltage of SCIG reduce with increase in rotor speed of turbine [11].

3. Simulation and Results

3.1 Simulation Model

A Simulation model was created in MATLAB Simulink. Different blocks like PV array, SCIG, VSC, and Grid are available in Simulink Library. The Fuzzy logic MPPT system, control of VSC to operate in inverting mode and as reactive power compensator, and a wind turbine model was modeled in the Simulnik with respective mathematical modeling. Overall system was developed by integrating those components. Active load of 50kW is connected to the grid through load bus.

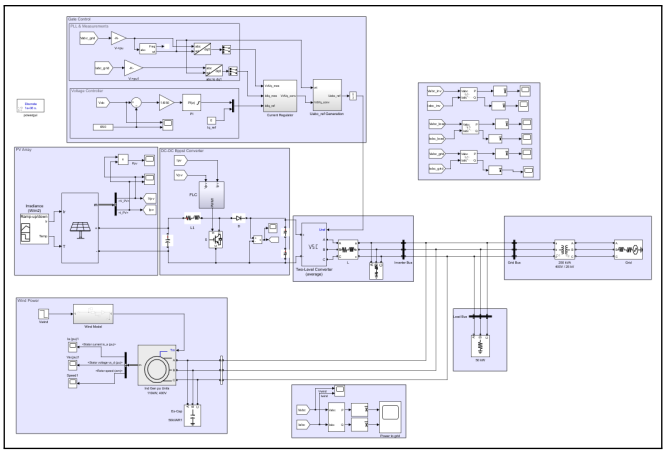

Figure 10: Simulation model with active load

3.2 Results

A MATLAB Simulink model of the whole system is developed and simulated using ode23t solver. The voltage level, current, active power, reactive power flow of PV-STATCOM, Wind Plant, Load bus and Grid bus are the main parameters that are analyzed in this section.

3.2.1 PV Plant

Irradiance and temperature are the input parameter while current, voltage and power are the output parameters that are taken in PV Plant. Changing irradiance level and constant temperature are considered in this analysis. When irradiance level was 1000W/m2 and temperature was 20°C the output voltage of PV plant was 279V, current was 360A and output power of PV-Plant was 100kW. When irradiance dropped to 250 Watt/m2 at 1sec to 1.8 sec, current was highly affected while voltage was slightly affected. So the output power was around 25kW. The transients seen at 4.2sec was due to increase of wind speed to 15m/s.

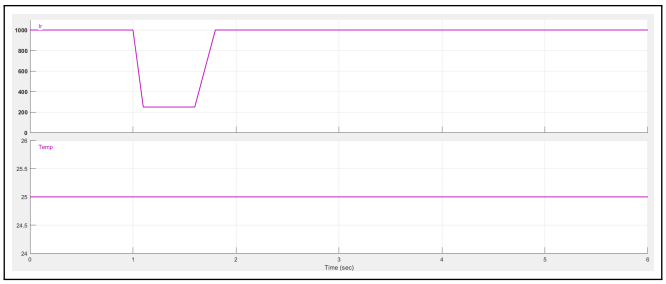

Figure 11: Input Irradiance (watt/m2) and Temperature (°C)

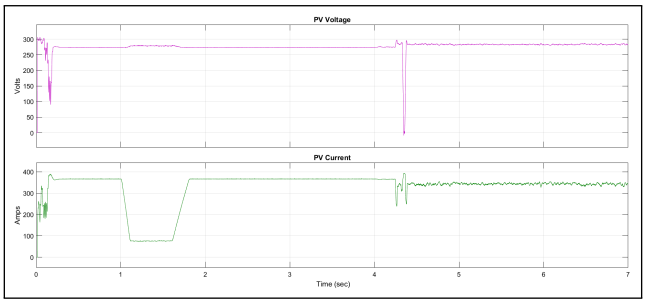

Figure 12: PV Array Voltage and Current

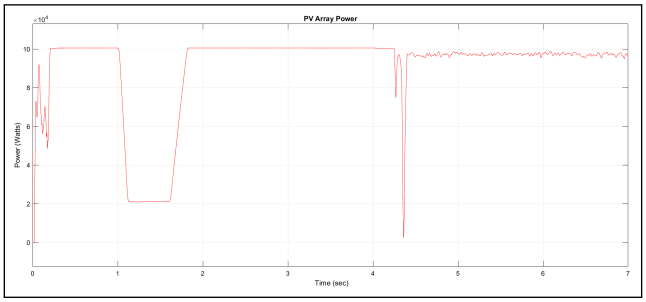

Figure 13: PV Array Output Power

3.2.2 Boost Converter and FLC

Considering boost converter to boost the output voltage of PV array and an interface between PV plant and load/grid, with Fuzzy logic as MPPT algorithm, DC link voltage was 650V initially, when wind speed was increased, DC link voltage increased to 2600V. The input voltage to the boost converter was 279V from PV Array.

Taking PV-Array current, voltage and power as input variables, FLC generated the duty cycle for boost converter whose value range from 0 to 1. Above figure is the magnified version of actual graph obtained. The frequency of obtained signal is 500Hz.

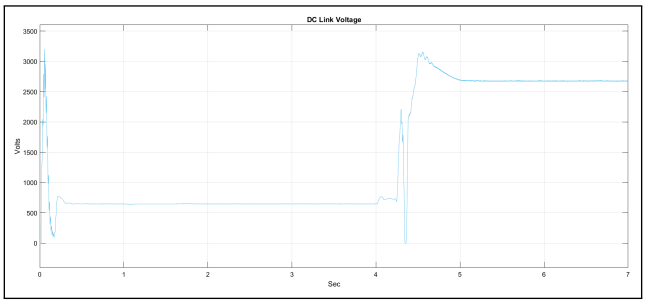

Figure 14: DC Link Voltage

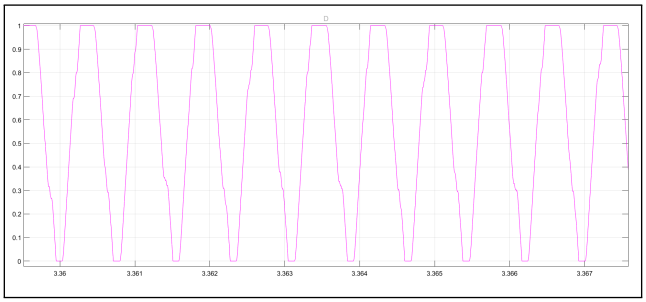

Figure 15: Gate signals generated from FLC to Boost Converter

3.2.3 Wind Plant with SCIG

Considering sweep radius of wind turbine to be 14 m and supplying constant wind speed of 9m/s for first four second and then stepped up to 15 m/s. The stator current and stator voltage of SCIG was 1 p.u., and rotor speed was around 1 Wm (rad/s) as shown in figure. But after 4 sec, stator voltage current and rotor speed varied too much. This might be due to absence of wind plant voltage controller.

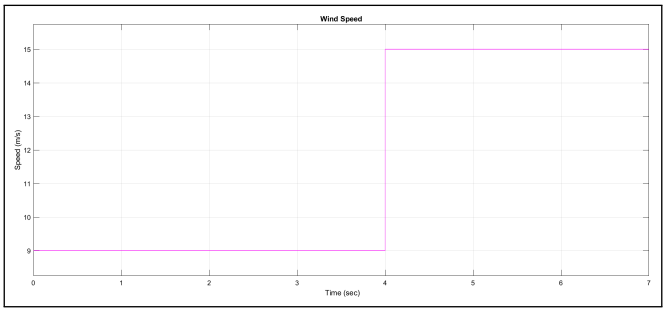

Figure 16: Wind Speed as input to wind plant

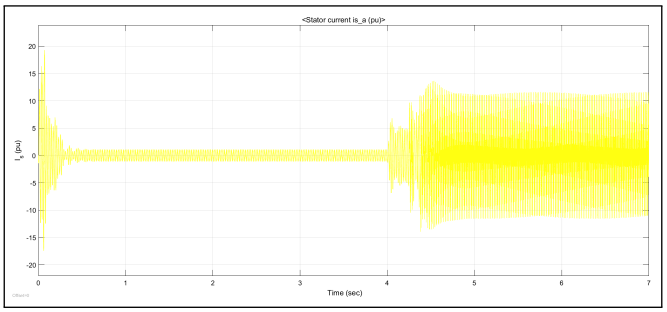

Figure 17: SCIG Stator Current

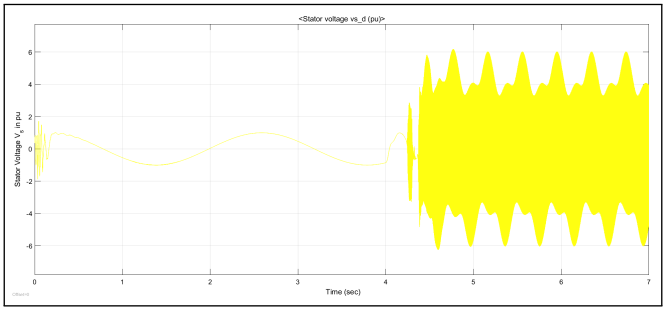

Figure 18: SCIG Stator Voltage

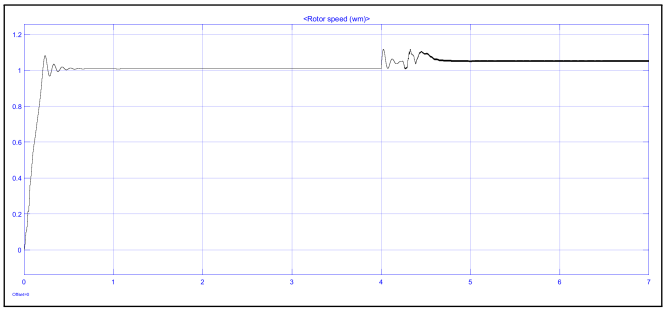

Figure 19: SCIG Rotor Speed

The power output of the wind plant at no reactive power loading was 110kW at the wind speed of 9m/s. When wind speed was increased to 15m/s, active power increased to 415kW and reactive power consumption was 6.5MVAR. Initially, the reactive power was supplied by external capacitor to the IG.

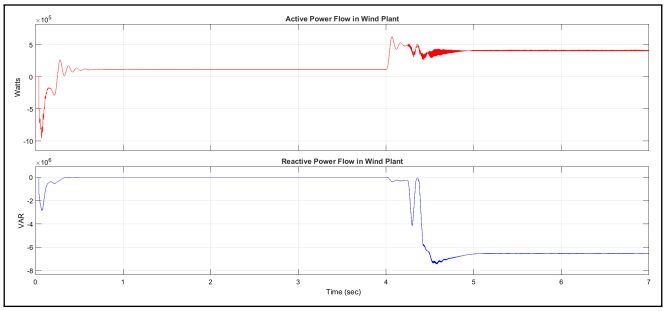

Figure 20: Power Flow in Wind Plant

Since, only PV plant is connected to the generator side of the inverter, the inverter power characteristics matches with the PV Plant output power. Output power decreased when the irradiance is decreased. For first four second, when wind speed was 9m/s, active load of 50kW is only connected so the reactive power of load is negligible. Active Power generated by PV Plant was 100kW and Wind Plant generated 110kW. The excess active power i.e., 160kW was supplied to grid while no reactive power was supplied. So the total generation was 210kW. Hence the active power is balanced among the system. When wind speed was stepped up to 15m/s, active power of wind increased to 113kW while load active power was also increased. Grid started consuming active power.

3.2.4 Comparison of existing system with system with PMSG

Wind plant with SCIG and PMSG is compared in this section. PMSG is connected to the system through back to back converter. Wind speed for PMSG is considered to be 10m/s and 12m/s. Figure below shows the active power flow in the system among Grid, PV inverter, Wind plant and load. The active power demand and supply is balanced among them. Demand by load is fulfilled by inverter and wind plant. Excess power is supplied to grid. 96kw is generated from PV-Plant while active load is increased from 100kw to 130kW. Wind plant generated 200kW at 10m/s and 340kW at 12m/s. Reactive power is also generated by the PV-STATCOM which is supplied to the connected load. The PMSG demand the reactive power which is supplied by grid. Load of 15kVAR is connected at 2.5 sec and again 15kVAR is added to make it 30kVAR at time 3.8 sec. PV-STATCOM supplied reactive power to those demand as shown in figure below. Reactive power demand by PMSG is around 200kVAR that is supplied by grid. In PMSG system, inverter controlling is done with Hysteresis band controlling technique. In this method, This method involves establishing a reference current as the desired ideal level and defining a hysteresis band around it. A relay is configured with threshold values of 0.1 and -0.1, which form the boundaries of this band. The relay monitors whether the injected current stays within these bounds and generates control signals for the IGBT switches in the inverter. If the actual current falls below -0.1, the relay produces an output of 1, while if it exceeds 0.1, the output is 0. This approach

ensures that the inverter current closely tracks the reference current within the specified thresholds [12].

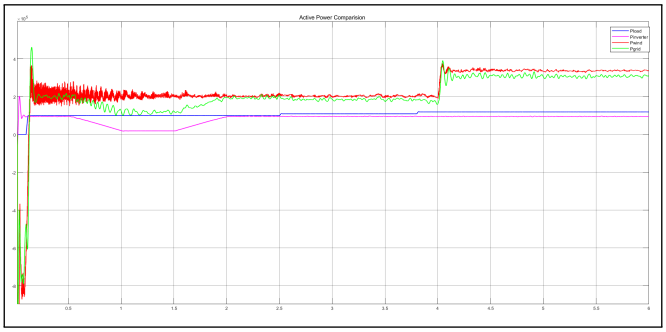

Figure 21: Active Power Flow in the system

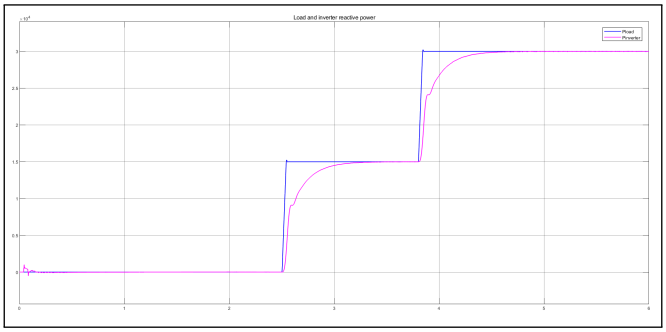

Figure 22: Reactive Power Flow between load and STATCOM

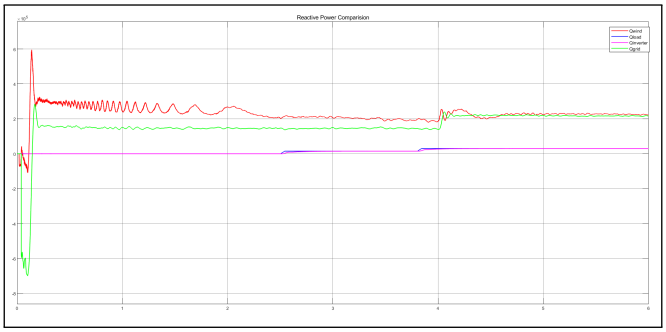

Figure 23: Reactive Power Flow in the system

4. Conclusion

PV Array of 100kW is integrated into a grid via boost converter and PV-STATCOM. Fuzzy logic controller is implemented to generate duty cycle of the converter. VSC is implemented as a PV-STATCOM where control logic for it is generated by modeling the signal generator. A SCIG of 110kW is also used and connected directly to the grid. The grid of 100MVA is considered in the project and excess power (160kW) is given to grid . From the above results, active power are generated and supplied to load and grid while reactive power is negligible due to active load only. Active power demand and supply is balanced. Reactive power compensation and power flow is seen to be better in PMSG system due to back to back converter that controls voltage level of wind plant.

References

[1] G. L. Pearson. *Bell Labs Solar Battery*. Bell Labs Record, 1956.

[2] M. Green, E. Dunlop, J. Hol-Ebinger, M. Yoshita, N. Kopidakis, and X. Hao. Solar cell efficiency tables (version 61). 2021.

[3] International Energy Agency (IEA). *Renewables 2021: Analysis and Forecast to 2026*.

[4] S. Bacha, D. Picault, B. Burger, I. Etxeberria-Otadui, and J. Martins. Photovoltaics in microgrids: An overview of grid integration and energy management aspects. 2015.

[5] P. Kundur. *Power System Stability and Control*. McGraw-Hill, 1994.

[6] N. G. Hingorani and L. Gyugyi. *Understanding FACTS: Concepts and Technology of Flexible AC Transmission Systems*. Wiley-IEEE Press, 1994.

[7] A. Hayat, D. Sibtain, A. F. Murtaza, S. Shahzad, M. S. Jajja, and H. Kilic. Design and analysis of input capacitor in dc–dc boost converter for photovoltaic-based systems. 2023.

[8] C. R. Algarín, J. T. Giraldo, and O. R. Álvarez. Fuzzy logic based mppt controller for a pv system. 2017.

[9] I. Tamrakar, K. Joshi, P. Karki, S. Bimali, and T. Aryal. Implementation of solar-pv inverter as statcom during nighttime in grid-connected system (pv-statcom). 2019.

[10] R. Jayathilake and P. Wijetunga. Design of wind turbine. 2015.

[11] M. H. Granza, H. Voltolini, J. Ivanqui, and P. L. K. Miranda. Wind power generation control system with squirrel cage induction generator. 2014.

[12] L Timilsina, P Acharya, RP Jnawali, S Paudel, I Tamrakar, and NP Gyawali. Universal power converter for microhydro power plant. 2016.